

Directed percolation effects emerging from superadditivity of quantum networks

L. Czekaj,^{1,2} R. W. Chhajlany,^{3,1,2} and P. Horodecki^{1,2}

¹*Faculty of Applied Physics and Mathematics, Gdańsk University of Technology, 80-952 Gdańsk, Poland*

²*National Quantum Information Center of Gdańsk, 81-824 Sopot, Poland*

³*Faculty of Physics, Adam Mickiewicz University, Umultowska 85, 61-614 Poznań, Poland*

(Dated: August 1, 2018)

Entanglement induced non-additivity of classical communication capacity in networks consisting of quantum channels is considered. Communication lattices consisting of butterfly-type entanglement breaking channels augmented, with some probability, by identity channels are analyzed. The capacity superadditivity in the network is manifested in directed correlated bond percolation which we consider in two flavours: simply directed and randomly oriented. The obtained percolation properties show that high capacity information transfer sets in much faster in the regime of superadditive communication capacity than otherwise possible. As a byproduct, this sheds light on a new type of entanglement based quantum capacity percolation phenomenon.

Introduction. Percolation (see *e.g.* [1, 2]) is a natural concept that emerges in the description of spreading processes in the presence of medium imperfections. Percolation effects in quantum networks have recently been the subject of increasing interest [3–7]. Most of the attention has been restricted to the generation of large scale networks with maximally entangled states between elementary nodes to allow for quantum communication applications, starting from initial imperfect, *i.e.* non-maximally entangled state networks. The interesting central new insight introduced in [3, 4] is that local quantum operations may be used not only to purify entanglement but, simultaneously, to change the topology of the lattice to a new one with lower percolation probability threshold. This idea has been developed for different states [5, 6] and lattice dimensions [7, 8]. In a different context, percolation concepts also appeared in quantum information theory (QIT) in the study of cluster state generation [9].

The capacity of a network determines its utility in the domain of communication. The development of QIT has led to the uncovering of interesting quantum effects on channel capacities, *e.g.* superadditivity of quantum (Q-type) channel capacity [10]. This result followed the intuition developed in the bound entanglement activation effect [11] (where two weak resources activate each other becoming collectively useful for some task) continued further in Refs. [12] and [13]. Independently, the first superadditivity effect of classical (C-type) capacity in quantum multi-access channels has been described [14]. Both Q-type and C-type superadditivities have been proven even for entanglement breaking channels [15].

In this paper, we consider percolation effects in quantum networks from a channel perspective. In particular, we show that channel superadditivity can be used to enhance percolation of information through networks. The schemes are based on network models of classical information transfer through quantum multipartite channels (MACs), which can be mapped to certain types of *directed* bond percolation problems [16]. We first consider a simple layered communication scheme (A) to demon-

strate the basic idea of percolation assisted by superadditive capacities and then describe a more complicated scheme of multidirectional communication (B). Interestingly, the percolation problem in case B does not seem to have been studied elsewhere in the literature.

The basic ingredients of the quantum networks are: a *passive* fixed underlying network built up of elementary entanglement breaking MACs, and an *active* auxiliary incomplete network consisting of randomly generated (open) bonds. The term passive means that no bond in the network allows *a-priori* high capacity communication (HCC), whereas elements of the active network are high capacity channels. Importantly, the active channels can serve to activate HCC through the passive channels.

Model A - Layered network communication. The elementary channel of the passive network is chosen in this paper as a 2-sender 1-receiver *noisy* quantum MAC depicted as the wedge shaped channels in Fig. 1(b): the slanted line is a two-qudit (d^2 -dimensional) input pertaining to one user; the vertical line is a single qudit input of the second user. The single qudit system is modified by one of a chosen set of (orthogonal) d^2 unitary operations fired by the logical value of the two-qudit system (see Ref. [15] for details). This single qudit line is further modified by a depolarizing channel and is the sole output system at the receiver's end. For moderate to large depolarization – the working regime considered here – this channel has poor classical capacity C' for any user [15]:

$$C' \ll C_0 \leq C_{\max} \equiv \log_2 d, \quad (1)$$

where C_{\max} is the maximal attainable capacity for a single qudit output, corresponding to an identity channel. Communication can be improved by adding a high capacity active channel, *e.g.* an ideal channel, along the vertical transmission line. Inputting a two-party maximally entangled state to the ideal channel and vertical line of a wedge channel increases the capacity along the slanted line of the wedge channel to a much higher value C_0 (see Eq.(1)) – a manifestation of superadditivity of channel capacities [21] (for high depolarization when the

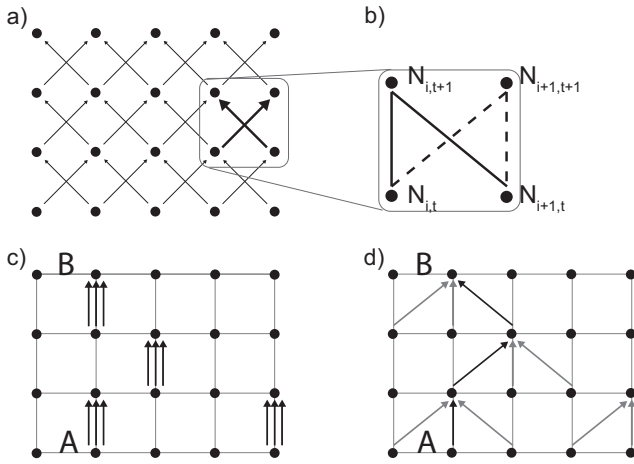


FIG. 1. Model A - layered communication network: a) passive network; users are located at nodes of a square lattice, the lattice is filled with butterfly shaped primitives, information flow is directed from layer $t \rightarrow t+1$; b) butterfly primitive consists of two MACs (solid and dashed wedges) from Ref. [15]; Node (user) $N_{i,t}$ can communicate with $N_{i-1,t+1}, N_{i,t+1}, N_{i+1,t+1}$ with maximal capacity $C' \ll C_0$; c) active network filled randomly by triples of ideal channels allowing HCC (no HCC from A to B); d) using entanglement changes the geometry of the HCC network leading to directed communication paths (black arrows) with capacities $\geq C_0$ from A to B.

channel becomes entanglement breaking, $C_0 \approx (d+1)C'$ [15]). We define HCC as transmission at a rate $\geq C_0$.

The structure of the wedge channel induces a sense of direction of communication. In the network context, we first consider the scenario where only forward communication is allowed (see Fig.1). The passive channel inputs are shared by nearest neighbour pairs of sites in horizontal layers giving rise to a butterfly shaped fixed network. The active channels are only placed on vertical bonds. Suppose that these are available with probability p – one can assume that identity channels are initially available at all vertical bonds, yet due to fragility w.r.t. noise either remain useful (ideal) with probability p or become unuseful random operations with probability $1-p$ effectively erasing information. In our scheme, we consider a setup where a triple of identity channels is the basic active channel [22]– this allows the possibility of simultaneous HCC between a given sender and his vertically placed receiver as well as between the sender's two horizontal nearest neighbours and that receiver (Fig. 1).

The question of establishing long range HCC in such a network is a directed percolation problem. One asks, under what conditions, is it possible for any user to be able to perform directed HCC, through intermediate nodes, with a user or users located at a distance scaling with the length of the network. One may compare two scenarios - (a) entanglement-free or classical, where no entanglement is allowed in the protocol used at any node and (b) entanglement-assisted (EA), which takes full ad-

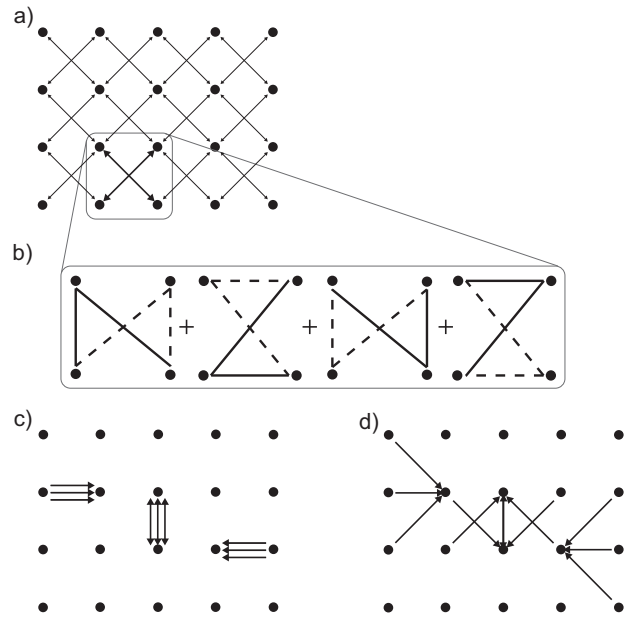


FIG. 2. Model B - Multidirectional communication networks: a) passive network, allowing communication in each direction; b) structure of butterfly primitive; c) active channels; d) emerging network geometry induced by entanglement between active and passive channels.

vantage of the superadditive effect described earlier. The former case corresponds to communication only along 1–dimensional paths and the percolation threshold probability is 1, rendering the network useless for HCC for finite loss probability of active channels. The EA scheme involves changing the geometry of the HCC network and is mapped to a *correlated* directed bond percolation problem where with probability p three directed bonds (forming an arrow shape) are placed on the lattice (Fig.1(e)). The threshold probability is significantly suppressed due to entanglement induced increased connectivity. We performed a standard Monte Carlo simulation (see [23]) and found the percolation threshold to be $p_c = 0.5388$ with accuracy $\Delta = 0.0005$. We have checked that the studied percolation transition lies, as expected, in the Directed Percolation (DP) universality class, by computing a complete set of critical exponents and found them to be in agreement with those obtained for the uncorrelated directed bond percolation problem. The important basic characteristic of directed percolation is that the connected clusters of nodes are geometrically highly asymmetrical and are restricted to acute cones (with cone angle $\pi/2$ when $p = 1$) with axes along the vertical lines passing through the starting nodes. Near the critical point the clusters are very narrow and essentially quasi 1-dimensional, as the probability of obtaining a connection with a site a large distance away from the source and at an angle θ from the axis, $\Theta(p, \theta) > 0$ for $|\theta| < \delta\theta(p) \sim (p - p_c)^b$ (see *e.g.* Dhar and Barma [17]).

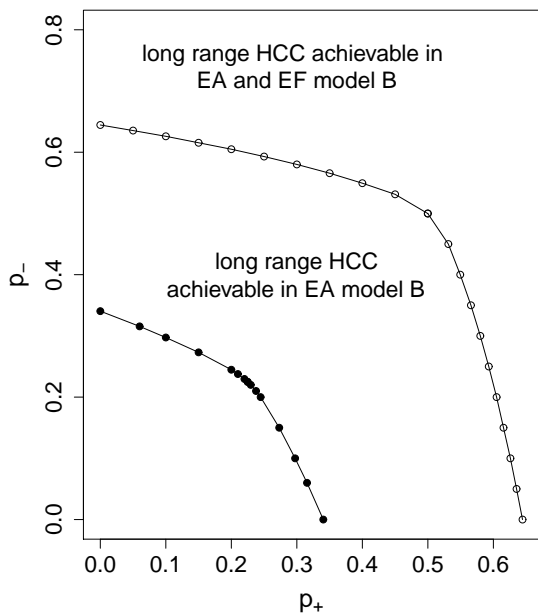


FIG. 3. (a) Comparison of the percolation critical lines (p_+^c, p_-^c) for percolation process on randomly oriented square lattice (classical scheme) and butterfly network (EA scheme). Dots are numerically obtained points.

The EA scheme beats the classical scheme in that there is a wide window in p for HCC, and that the horizontal extent of connections $|\theta|$ at a distance $t \rightarrow \infty$ away changes from 0 to $\pi/4$ as p increases from p_c to 1.

Model B – Randomly oriented communication. We now move to a general scenario within the described framework of channels (Fig. 2). Now each node can communicate in *both* directions with its nearest neighbours (main bonds) on a square lattice as well as all of its next nearest neighbours (diagonal bonds) through the passive network. The configuration leading to this possibility is shown in Fig.2 (a) and (b). The active network channels are placed along the main bonds of the square lattice and are tagged for use in a particular direction.

HCC between distant nodes is now a multidirectional bond percolation problem. We consider the case where upward, left-to-right oriented identities are present with probability p_+ while downward, right-to-left oriented identities are placed with probability p_- . Note, that bidirectional bonds appear as the independent choice of two oppositely directed channels on a given bond.

This setup is interesting already for the case when, say, $p_+ = 0$. Using an entanglement free protocol, capacity $C \geq C_0$ can already be obtained through the main bonds of the square lattice along the up or right directions, in contrast to Model A. This is the well known square lattice directed bond percolation problem for which the percolation threshold $p_c \approx 0.64$ (see *e.g.* [17]). But, in the EA scheme, due to increased and correlated connectivity, the

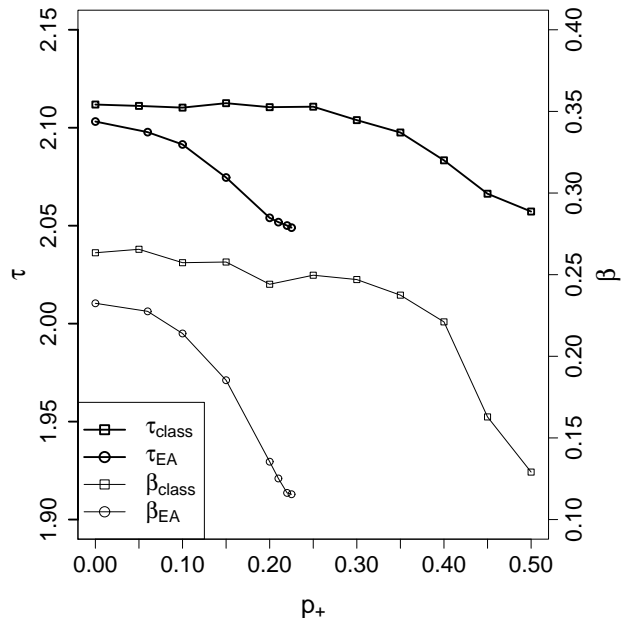


FIG. 4. Comparison of critical exponents τ, β for classical and EA schemes of multidirectional oriented percolation.

percolation threshold is almost halved w.r.t. the classical scheme and has been calculated here to be $p_c \approx 0.34$. Both phase transitions lie in the DP universality class. At moderate $p \approx 0.6$, the probability of a starting node belonging to an infinite or system spanning anisotropic cluster (in the thermodynamic limit) $F_\infty > 1/2$ using superadditivity effects while $F_\infty = 0$ otherwise.

The general multidirectional communication problem is the most interesting setup. In the classical scenario, this reduces to square lattice randomly oriented percolation. Problems of this category were studied in the context of random resistor diode networks (see *e.g.* [19]) mainly using renormalization group calculations. However not many results seem to be available in the literature on the p_\pm percolation problem (see however [20] for some analytical properties).

Here, we map out the phase diagram in the (p_+, p_-) plane in Fig.3 using Monte Carlo simulations (see Appendix). Note that the diagram is symmetrical w.r.t. the line $p_+ = p_-$ due to system symmetry under the interchange $p_+ \leftrightarrow p_-$. This result is to be compared with the multidirectional correlated bond percolation phase diagram for the EA scheme (Fig. 2(d)). As can be seen in Fig.3, the EA scheme is drastically better than the classical scheme in the whole parameter plane.

An interesting feature of both schemes is that they allow switching of universality classes of phase transitions from the DP class to the Isotropic Percolation (IP) class to which standard bond/site percolation belongs. This is facilitated by the choice of parameters p_\pm , and as a result one may accordingly change the properties of the

long range clusters. To provide evidence for this, we calculate two universal critical exponents (Fig. 4) β and the Fisher exponent τ (see [23]) as one moves along the critical lines (Fig. 3) of the two models. Recall, that β determines how the percolation probability $F_\infty \sim (p-p_c)^\beta$ increases above the percolation threshold, while the Fisher exponent determines how the probability of obtaining a cluster larger than size n decreases with n at the critical point $p = p_c$: $F_n \sim 1/n^{\tau-2}$. Note that the values of these exponents in the DP class are $\beta \approx 0.276, \tau \approx 2.112$ [17] and in IP: $\beta = 5/36 \approx 0.139, \tau = 187/91 \approx 2.0549$ [1]. First consider square lattice multidirectional percolation in Fig.4 (the classical scheme). Both exponents show that as one moves along the critical line, the phase transitions lie in the DP universality class until $p_-^c \approx 0.4$, since this region inherits the exponents at the DP point $p_-^c = 0$. At $p_-^c = 1/2 (= p_+^c)$, which is an isotropic symmetry point, one obtains values of the exponents corresponding to the IP universality class. In between, there is a characteristic crossover region between the two types of behaviour. In particular, this means that for a choice of parameters approaching the isotropic point, one obtains different characteristic growth of clusters (determined by different critical exponents) than when in the DP region. Secondly the cluster geometrical characteristics change from highly anisotropic to isotropic. The butterfly network percolation problem (EA scheme) basically follows the same pattern (see Fig. 4) and can be considered a rescaled version of the classical problem, wherein again lies the quantum advantage of the EA scheme. For this network, the isotropy point is found to be located at $p_+^c = p_-^c \approx 0.225$. The slightly lower values of β in the DP regime as compared to the square lattice problem do not seem to be significant - and are a result of the extreme sensitivity of the calculated exponents on the accuracy of critical probabilities.

Concluding remarks. We have described percolation effects in a channel context showing how directed percolation effects (not considered before) emerge in the consideration of quantum networks. In the context of percolation theory, to our knowledge, the multidirectional correlated bond percolation problem has not been studied before. Finally, quite remarkably, our results provide a new entanglement percolation effect in the spirit of Ref. [3]. Keeping everything else unchanged, consider the Bell measurement (BM) channel of Fig. 1 of Ref. [15] instead of the MAC used here, with AC (BC) playing the role of diagonal (resp. vertical) bond of the square lattice. Then any randomly generated singlet between B and C can be switched, via entanglement swapping, to a singlet on the diagonal AC. This leads to the same geometry as discussed here but now one asks about the possibility of building a long range network of singlets. Note that singlets are directionless. Without using the BM channel, we obtain a “classical” scheme related to square lattice percolation which has threshold $p_c = 0.5$. Since direc-

tionless percolation must certainly be at least as good as directed percolation, an EA scheme making use of the switching mechanism of the BM channel will have threshold at most equal to the calculated threshold at the isotropic point of Model B $p_c^{\text{EA}} \leq p_+^c = p_-^c \approx 0.225$.

The authors thank J.K. Korbicz for discussions. P. H. thanks also C. H. Bennett and A. Grudka for discussions. The work was supported by EU project QESSENCE and by the Polish Ministry of Science and Higher Education through Grant No. NN202231937. Part of the work was done in Quantum Information Centre of Gdansk.

-
- [1] D. Stauffer and A. Aharony, Introduction to percolation theory, Taylor & Francis 2003.
 - [2] G. Grimmett, Percolation, Springer-Verlag 1999.
 - [3] A. Acin, J. I. Cirac, and M. Lewenstein, Nature Phys. **3**, 256 (2007).
 - [4] G. J. Lapeyre, Jr., J. Wehr, and M. Lewenstein, Phys. Rev. A **79**, 042324 (2009).
 - [5] S. Perseguers, L. Jiang, N. Schuch, F. Verstraete, M. Lukin, J. Cirac, and K. Vollbrecht, Phys. Rev. A **78**, 062324 (2008); S. Perseguers, D. Cavalcanti, G. J. Lapeyre, Jr., M. Lewenstein, and A. Acin, Phys. Rev. A **81**, 032327 (2010).
 - [6] S. Broadfoot, U. Dorner, and D. Jaksch, EuroPhys. Lett. **88**, 50002 (2009).
 - [7] S. Perseguers, Phys. Rev. A **81**, 012310 (2010).
 - [8] A. Grudka *et al.*, manuscript in preparation (2011).
 - [9] K. Kieling, J. Eisert, „Percolation in quantum computation and communication”, in: *Quantum and Semi-classical Percolation and Breakdown in Disordered Solids*, pages 287-319 (Springer, Berlin, 2009).
 - [10] G. Smith, J. Yard, Science **321**, 1812 - 1815 (2008).
 - [11] P. Horodecki, M. Horodecki, R. Horodecki, Phys. Rev. Lett. **82**, 1056 (1999).
 - [12] P. Shor, J. A. Smolin, and A. V. Thapliyal, Phys. Rev. Lett. **90**, 107901 (2003).
 - [13] W. Duer, J. I. Cirac, and P. Horodecki, Phys. Rev. Lett. **93**, 020503 (2004).
 - [14] L. Czekaj and P. Horodecki, Phys. Rev. Lett. **102**, 110505 (2009).
 - [15] A. Grudka and P. Horodecki, Phys. Rev. A **81**, 060305(R) (2010).
 - [16] S. R. Broadbent and J. M. Hammersley, Proc. Camb. Phil. Soc. **53**, 629 (1957).
 - [17] D. Dhar and M. Barma, J. Phys. C: Solid State Phys., **14**, L1 (1981).
 - [18] H. Hinrichsen, Adv.Phys. **49**, 815 (2000).
 - [19] S. Redner, J. Phys. A: Math. Gen. **14**, L349 (1981); *ibid* **15**, L685 (1982); Phys. Rev. **B 25**, 3242 (1982).
 - [20] Geoffrey R. Grimmett, Random Structures & Algorithms **18** 257 (2001)
 - [21] This is a superadditive effect as the identity is unavailable to the user of the slanted input line of the wedge channel.
 - [22] For qubit channels, *e.g.* this can be physically realized as a process of ideal transmission with probability p of a single photon having three frequency states and two polarization degrees of freedom for each frequency, where the dominating noise process is photon loss.

[23] See supplemental material for methods.

Directed percolation effects emerging from superadditivity of quantum networks

Lukasz Czekaj, Ravindra W. Chhajlany and Paweł Horodecki

Methods

The critical percolation properties of the two models were studied using direct Monte Carlo simulations in the spirit of Dhar and Barma [1]. We studied the change in behaviour of the probability F_n , of appearance of clusters of size greater than n , with bond probabilities p and looked for characteristic scaling behaviour expected in the critical region to identify percolation thresholds plotted. Below the probability threshold, $F_n \propto \exp(-n)$ for large n while $F_n \rightarrow \text{constant}$ in the supercritical phase [1]. The critical region is characterized by scaling laws with $F_n \propto n^{2-\tau}$ described by a power law dependence at the critical value p_c , which we localized by sweeping through super- and sub-critical probabilities using an interval bisection method. For model A, cluster size distribution data was obtained by performing 10^5 realizations (per value of probability p) of cluster growth starting from a single node. Model B simulations were performed on a fixed 2×10^3 by 2×10^3 square lattice also with 10^5 realizations for each p , where cluster connectivity was identified using a breadth-first search algorithm.

The qualitative values of the critical exponents τ, β presented in the paper for model B are defined as follows:

$$F_n(p) \sim n^{-(\tau-2)} \text{ at } p = p_c$$

and

$$F_\infty(p) \sim (p - p_c)^\beta$$

A simple method used to obtain these was to directly calculate the slope of the plots of these two functions in log-log scale. Since the problem contains two parameters p_+, p_- , we chose one of them p_+ do be the independent parameter with $p_-(p_+)$ determined so as to be on the critical line of the model. For the determination of β , we considered clusters of size n greater than 10^5 to be “infinite” or system spanning clusters on the finite lattice.

Alternatively, we also determined β from τ and an auxiliary exponent γ , which describes the critical behaviour of mean cluster size $\langle n \rangle$ also readily available from the simulation:

$$\langle n \rangle \sim (p_c - p)^{-\gamma} \text{ for } p - p_c \rightarrow 0^+$$

The following universal equation, derived from scaling relations, is known to hold for directed (uncorrelated) bond percolation [1] and isotropic percolation [2]:

$$\beta = \left(\frac{\tau - 2}{3 - \tau} \right) \gamma$$

We assumed the equation to be true for the entire critical plane and obtained results for β in agreement with those obtained using the first method. Results obtained in the latter manner are those presented in the paper.

[1] D. Dhar and M. Barma, J. Phys. C: Solid State Phys., **14**, L1 (1981).

[2] D. Stauffer and A. Aharony, Introduction to percolation theory, Taylor & Francis 2003.